

Abstract

Add a space

was undertaken

1  
2  
3

# COMPARISON OF INTERCONTINENTAL AEROSOLS: DESERT AND MONSOON-INFLUENCED REGIONS

## AIM:

This work is to compare the optical and physical properties of aerosols at 440nm, 675nm, 870nm and 1020nm spectral bands between Desert and Monsoon-influenced regions. In this work, Zinder and Beijing were chosen to represent desert and Monsoon influenced regions respectively.

## Place and Duration of Study:

Four years data of Aerosol Optical Depth (AOD) were extracted from level 2.0 quality assured almucantar version products of AERONET data, at both Beijing-CAM (116.317°E & 39.933°N) and Zinder Airport (8.984°E & 13.775°N) between 2012 and 2015.

## Methodology:

In this work, physical and optical properties of aerosols were determined using Angstrom equations. Angstrom exponent, Curvature, Turbidity coefficient and Spectral variation of the aerosols in each of Zinder Airport and Beijing-CAMP were determined and the results were then compared. Both the physical and optical properties of the aerosols were determined from the calculated values of Angstrom exponent, Curvature, Turbidity coefficient and spectral variation.

## Results:

The results obtained showed that there was dominant coarse-mode aerosols particles size in Zinder city, whereas domination of fine-mode aerosol particles in Beijing was found. The results also showed that the overall Aerosol Optical Depth (AOD) in Zinder is higher than that of Beijing, but the atmosphere of Beijing was hazier than that of Zinder.

## Conclusion:

The prevalence of coarse-mode particles size in Zinder was due to desert dust particles in the region, whereas the prevalence of fine-mode particles in Beijing was due to anthropogenic aerosol particles in the region, which may be resulted from heavy industrialization in China. The higher Aerosol loading in Zinder is responsible for absorbing light coming from the sun, which in turn makes the atmosphere clear, whereas the lesser aerosol loading in Beijing is responsible for scattering light coming from the sun, thereby obstructing the atmospheric visibility in the region.

Keywords: Angstrom exponent, Turbidity coefficient, Aerosol Optical Depth, Curvature, AERONET

## 1.0 Introduction

Apart from green-house gases, aerosol is another important agent of radiative forcing that affects the planet Earth [1-3]. Aerosol affects our environment [1-3], influences cloud formation [4], and causes overall increase or decrease in atmospheric temperature [5]. Aerosol also affects human health by penetrating deep down into respiratory and cardiovascular system [6, 7]. These effects of aerosol make it necessary to monitor it via both ground-based observation and satellite [4, 8, and 9]. However, it is difficult to monitor aerosol properties via satellite, because satellites always rely on backscattering

Note: directional coordinates should list latitude ~~then~~ longitude then as shown below.

(13.775°N, 8.984°E)

1

(39.933°N, 116.317°E)

them

ultimately the

calculated

Add a space

the

data

project

of

research project

while

lower

while

generation

while

were found

were

indicated



signals, which are more often than not contaminated signals [10]. This is the reason why ground-based measurements are more commonly used to get accurate aerosol data, since the ground-based instruments are mounted to take measurements directly facing the sun.

There are ~~numerous~~ <sup>a</sup> number of ground-based Sun-photometer networks across the globe that are used for aerosol monitoring. These include SKY-Radiometer network (SKYNET) and Aerosol Robotic Network (AERONET). AERONET is a very popular and reliable source of aerosol data. <sup>and</sup> It provides measurements <sup>add a space</sup> in over 400 data stations <sup>from</sup> worldwide for accurate retrieval of aerosol optical depth (AOD), single-scattering albedo (SSA), aerosol particle size distribution (PSD), by taking into account direct solar measurement and scattering measurement [14,15], <sup>AERONET</sup> and it became a yardstick for satellite AOD retrieval [16,17]. Two of the AERONET data stations are Beijing-CAM in China, and Zinder Airport in ~~Niger republic~~ <sup>the Republic of Niger</sup>.

Beijing is the capital city of China, <sup>and</sup> it is located in North-China, the East-Asian region, situated at longitude 116.317°E and latitude 39.9330N, with a population of more than 19 million [18]. Beijing <sup>is located in</sup> belongs to the warm temperate zone, half moist continental monsoon climate, featuring four distinct seasons: Arid multi-windy spring, hot and multi-rain summer, sunny and fresh autumn and <sup>Beijing</sup> the cold and dry winter, and has experienced rapid economic development over the past decades. Beijing shows distinct seasonal transitions. Atmospheric pollution is a ~~concerned~~ <sup>several</sup> problem in Beijing, <sup>because it affects</sup> due to human activities and frequent dust storm events in the city. Zinder, on the other hand, is one of the most popular cities in <sup>the</sup> Niger Republic. It is located at Longitude 8.984°E and Latitude 13.775°N in the West-African sub-region. It is typically characterized as a Sahara desert area, with virtually no rainfall. The arid nature of Zinder makes it possible for dust to prevail and <sup>is triggered by</sup> likely to cause haze in the atmosphere. Figures 1a and 1b respectively depict Beijing and Zinder <sup>study was designed</sup> cities.

This <sup>collected</sup> study intends to find correlation between aerosol particle size distribution, (PSD), aerosol optical depth, (AOD), and atmospheric visibility in the two cities, using four years <sup>from</sup> worth of level 2.0 AERONET data in Beijing-CAM and Zinder airport <sup>between</sup> 2012 to 2015.



Figure 1a: Map of Zinder



Figure 1b: Map of Beijing

## 2.0 Material and Method

Four years (2012-2015) of level 2.0, 'the quality-assured' AOD data <sup>from</sup> each of Zinder and Beijing were extracted from <sup>the</sup> AERONET database using <sup>the</sup> standard retrieval procedure <sup>for</sup> of AERONET products. These raw data archive files were unpacked using WinRAR 4.11 wizard, and viewed <sup>using</sup> through the Microsoft Excel ~~files~~ windows. The AOD data used were measured at four spectral bands, namely: 440nm, 675nm, 870nm and 1020nm.

Annual median averages of the AODs <sup>with</sup> alongside their corresponding wavelengths were computed and arranged in tabular forms. Statistical comparison between annual AOD in Zinder and that of Beijing was <sup>performed</sup> carried out.

The annual mean AODs of ~~both~~ Zinder and Beijing were plotted against their corresponding wavelengths and ~~the graphs~~ were fitted <sup>using</sup> on the second-order polynomial curve <sup>with</sup> in natural

equations for the graphs



63 logarithmic coordinates, using least square fitting procedure to determine the Angstrom coefficients for  
 64 in both Zinder and Beijing. The Angstrom coefficients determined were Curvature ( $\alpha_2$ ) and  
 65 Turbidity ( $\beta$ ). *AOD*

66 The Angstrom equation is given as:

$$67 \tau = \lambda^{-\alpha} \dots \dots \dots (1)$$

68 The linear equation that links the natural-logarithmic AOD and the corresponding  
 69 natural-logarithmic wavelength is:

$$70 \ln \tau = -\alpha \ln \lambda + \beta \dots \dots \dots (2)$$

71 The second order polynomial equation relating the AOD and the wavelength in natural  
 72 logarithmic form is:

$$73 \ln \tau = \alpha_2 \ln \lambda^2 + \alpha_1 \ln \lambda + \beta \dots \dots \dots (3)$$

74 Where:  $\tau$  is the AOD;  $\alpha_2$  is the curvature;  $\beta$  is the turbidity coefficient;  $\alpha$  is the Angstrom  
 75 exponent.

76 Angstrom equation was also employed to determine the annual Angstrom exponents  
 77 in each city. The expression for Angstrom equation is given as:

$$78 \alpha = - \frac{d \ln \tau}{d \ln \lambda} \dots \dots \dots (4)$$

79 Spectral variation of AOD ( $\alpha'$ ) was also determined using the ~~expression of the~~ second  
 80 derivative of Angstrom exponent ( $\alpha$ )

$$81 \alpha' = \frac{d \alpha}{d \ln \lambda} = -2 \alpha_2 \dots \dots \dots (5)$$

82 The values of  $\alpha_2$ ,  $\beta$ ,  $R^2$  and  $\alpha'$  were presented in a tabular form. Where:  $R^2$  is the least  
 83 square value of the residual.

### 84 3.0 Results and Discussions

85 Values of annual median AODs in both Zinder and Beijing at four different spectral  
 86 channels, from the year 2012 to the year 2015 were presented in table 1 below. The AODs  
 87 in each case decreased with corresponding increase in wavelength. This decreasing  
 88 trend of AOD with wavelength was presented in Figures 2a-2b. Figure 2a compares AODs  
 89 between Zinder and Beijing in 2012 at the four considered wavelengths. In each case, the  
 90 AOD in Zinder was higher than AOD in Beijing. At 440nm, the difference between Zinder  
 91 and Beijing AODs was 0.028 which is a reasonably small value. At 1020nm, however, the  
 92 difference in AODs in Zinder and Beijing was relatively high of value 0.126. This implies  
 93 that 1020nm channel showed highest difference in AOD, whereas 440nm channel showed  
 94 lowest difference in AOD in the two cities in the year 2012.

Wavelengths

between

between

4

displayed the

displayed the

add a space

are at

a

exponents

calculate

used

that were calculated

algorithm

calculate

for

95 In 2013, Zinder also showed higher AOD values in all considered spectral channels  
 96 except at 440 $\mu\text{m}$ . At 440 $\mu\text{m}$ , the AOD value in Beijing was 0.425, whereas that of Zinder  
 97 was 0.412. This implies that the AOD in Beijing at 440 $\mu\text{m}$  channel is higher by 0.013. At the  
 98 1020 $\mu\text{m}$  and 675 $\mu\text{m}$  respectively, Zinder showed highest and lowest values of AOD more  
 99 than Beijing with respective values of 0.307 and 0.357.

100 The case of year 2014 is similar to that of 2013. Value of AOD in Beijing at 440 $\mu\text{m}$  was  
 101 0.273, which was higher than that of Zinder (0.227) at the same spectral channel. The  
 102 difference was 0.046, which was more significant than that of 2013. However, AOD of  
 103 Zinder was higher than that of Beijing in the remaining three spectral channels in 2014.  
 104 The difference was highest at 1020 $\mu\text{m}$  with value 0.022, and lowest at 870 $\mu\text{m}$  with value  
 105 0.011.

106 In 2015, AOD in Zinder, was higher than that of Beijing throughout the spectral  
 107 channels. The differences were 0.149, 0.232, 0.243 and 0.241 at 440 $\mu\text{m}$ , 670 $\mu\text{m}$ , 870 $\mu\text{m}$  and  
 108 1020 $\mu\text{m}$  respectively.

109 Table 1: Annual Median AODs at Four Spectral Channels in Zinder and Beijing, 2012-  
 110 2015.

$\lambda$ ( $\mu\text{m}$ )	AOD (2012)		AOD (2013)		AOD (2014)		AOD (2015)	
$\lambda$ ( $\mu\text{m}$ )	Zinder	Beijing	Zinder	Beijing	Zinder	Beijing	Zinder	Beijing
111 0.440	0.386	0.358	0.412	0.425	0.227	0.273	0.442	0.293
112 0.675	0.301	0.208	0.357	0.247	0.171	0.160	0.406	0.174
113 0.870	0.260	0.152	0.324	0.196	0.140	0.123	0.380	0.137
114 1.020	0.243	0.117	0.307	0.173	0.124	0.102	0.360	0.119

Table 2: Angstrom Parameters in Zinder and Beijing, 2012-2015.

Year	$\alpha_2$		$\beta$		$R^2$		$\alpha$		$\alpha'$	
Year	Zinder	Beijing	Zinder	Beijing	Zinder	Beijing	Zinder	Beijing	Zinder	Beijing
2012	0.329	0.570	0.640	0.792	0.999	0.996	0.580	1.256	-0.658	-1.140
2013	0.154	0.844	0.561	0.988	1.000	0.995	0.354	1.135	-0.308	-1.688
2014	0.172	0.506	0.382	0.632	1.000	0.995	0.710	1.170	-0.344	-1.012
2015	-	0.540	0.502	0.663	0.998	0.996	0.222	1.115	-	-1.080



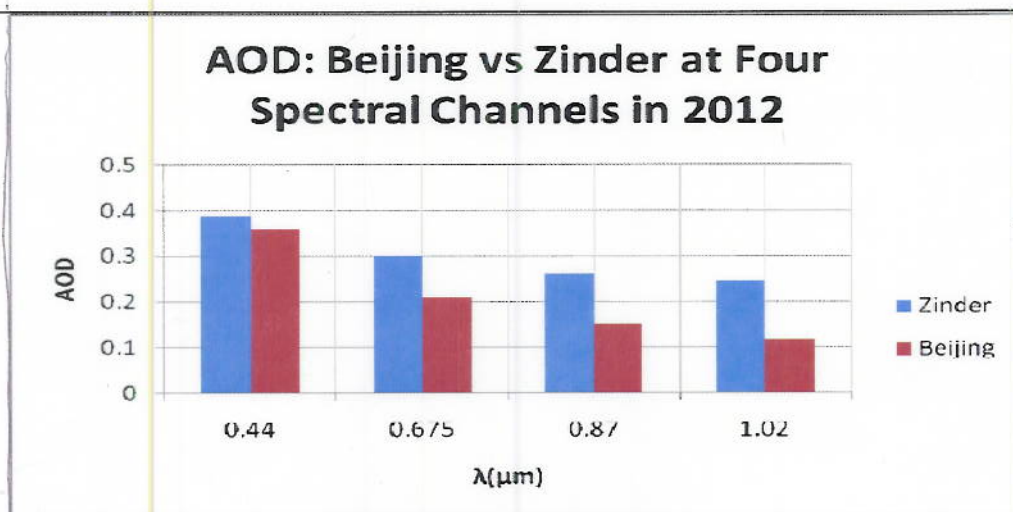


Figure 2a

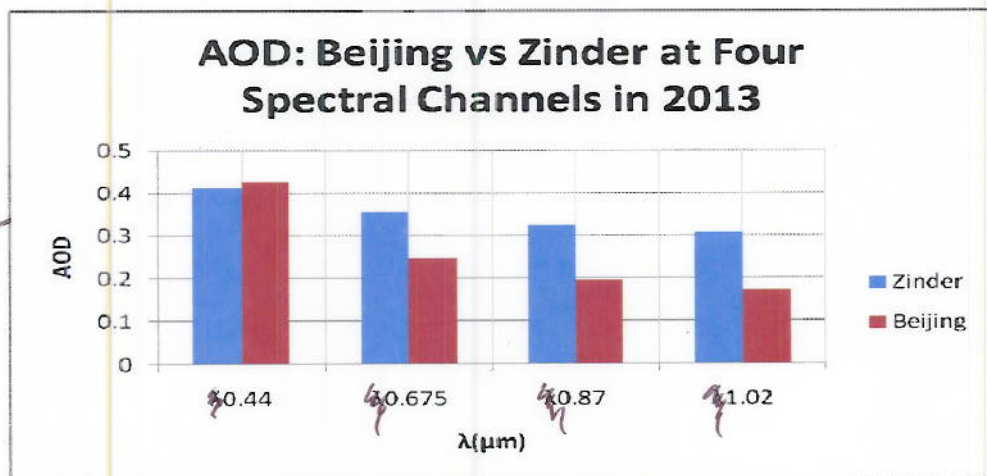
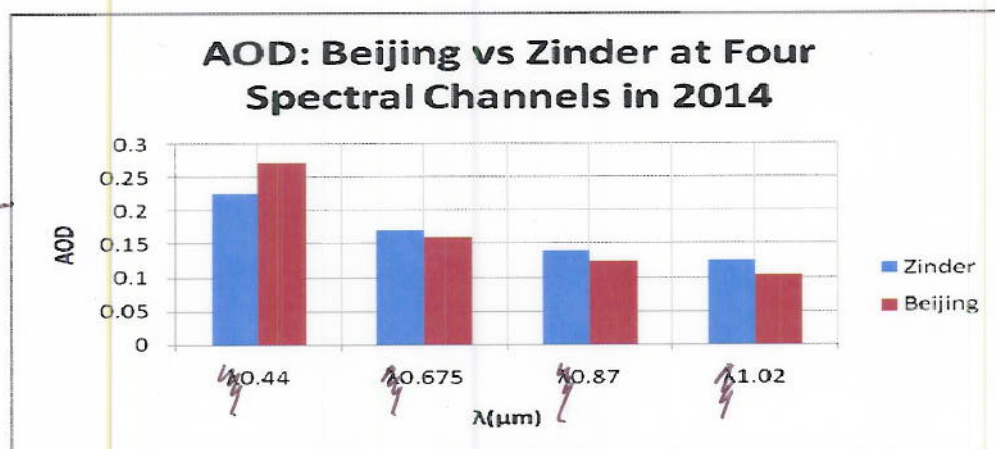


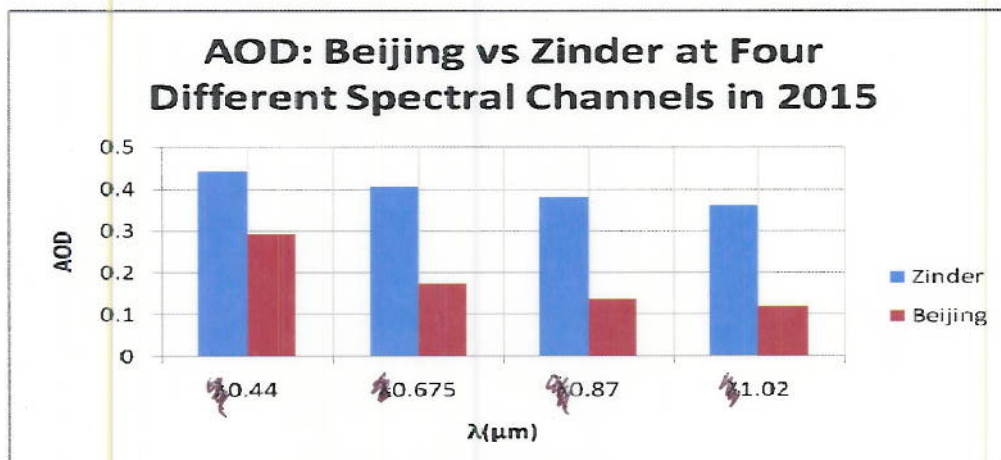
Figure 2b



*align figures to be the same width*

118

Figure 2c



119

120

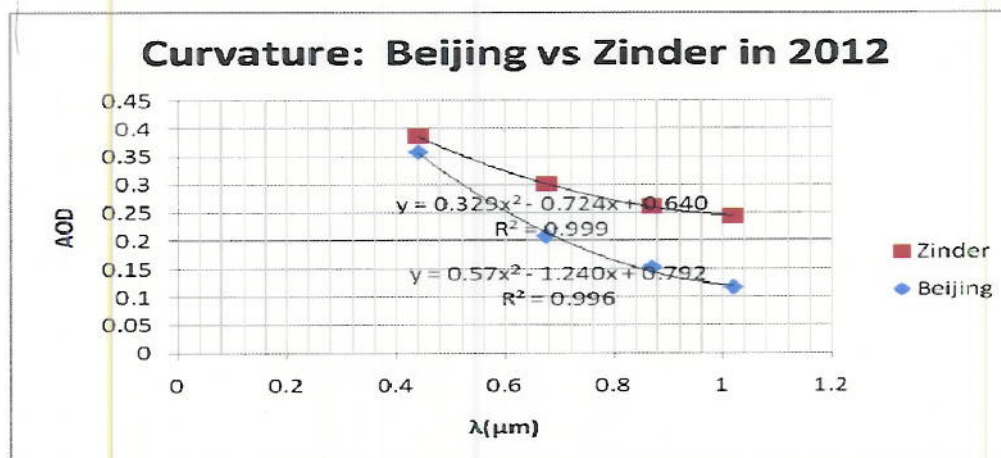
Figure 2d

121

122

Figure 2: Comparison of Annual AOD between Zinder and Beijing Cities

123



124

125

Figure 3a

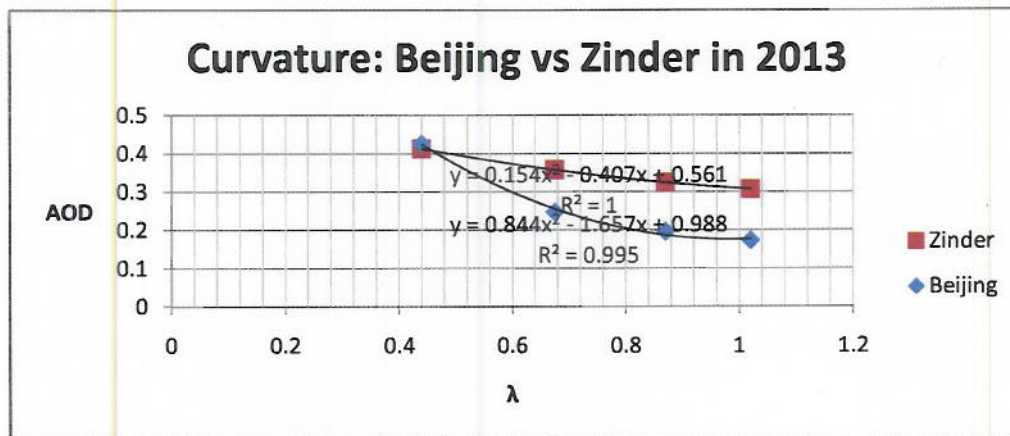


Figure 3b

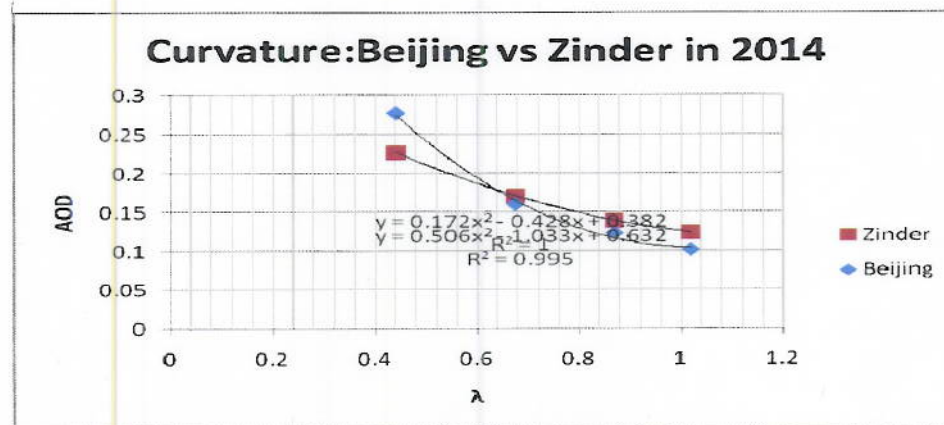


Figure 3c

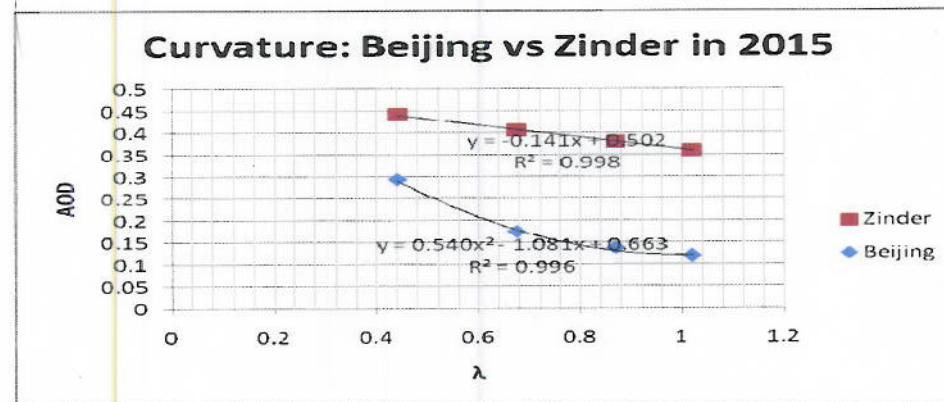


Figure 3d

Figure 3: Comparison of Curvature and Turbidity Coefficient between Zinder and Beijing Cities

Align figures to be the same width



Make  $\alpha$  symbol larger and more visible

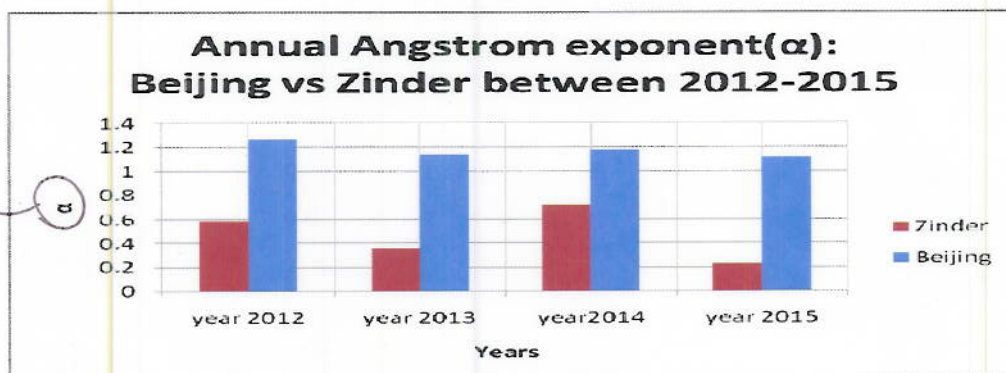


Figure 4: Comparison of Angstrom Exponent between Zinder and Beijing Cities.

With regard to particle size characterization in each city, although aerosol particles size can be determined using volume concentration in 22 radius bins, the angstrom exponent values were used instead as an index for the characterization. Conventionally, values of  $\alpha$  range are between zero to two (0-2); fine-modes of aerosol particles take values of  $>0.6$ , whereas coarse-modes take lesser values of  $<0.6$ . [11, 19 and 20]. From Table 2, all  $\alpha$ -values in Beijing were  $>0.6$ . This signifies the prevalence of fine mode particles in Beijing. In Beijing, fine mode fraction was larger than 50%, even more than 70% for summer [21]. Average  $\alpha$ -values in Beijing recorded in the year 2016 were from around 1.0 (1.1) in 2005 to around 1.1 (1.2) in 2014 [21]. This  $\alpha$ -value of 1.1 (1.2) in 2014 agrees very well with our value of 1.170 recorded in 2014. For Zinder, on the other hand,  $\alpha$ -values were  $<0.6$ . This implies dominance of coarse mode particles in the region. However,  $\alpha$ -value recorded in 2014 was 0.710, which indicates dominance of fine mode particles according to [22]. This might be due to error of instrumentation, meteorological factor or inadequacy of the Angstrom formula used in the calculation. However, it was reported that any value of  $\alpha$  in order of zero can be considered as coarse-mode [22]. So based on this report, this  $\alpha$ -value of 0.710 is considered as an indicator of coarse mode, mixed with reasonable amount of fine-mode particles. Thus domination of coarse mode particles in Zinder was due to the fact that Zinder is a Sahara region, which is typically characterized with dust aerosol. Comparison of Angstrom exponent between Zinder and Beijing was given in Figure 4. Moreover, studies show that curvature of coarse mode aerosol particles and that of bimodal aerosol particles, in which coarse mode is dominant, always appear positive; it changes rapidly with aerosol properties, and it affects the value of  $\alpha'$ . From Table 2, all  $\alpha_2$ -values were positive, which indicates prevalence of coarse mode particles in both Beijing and Zinder. However, curvature of  $\ln \tau$  versus  $\ln \lambda$  was found to be negative for biomass burning aerosols in Bolivia and Zambia, and for urban industrial aerosol in USA [22]. Based on this report, it is possible that fine-mode particles that were claimed to be of more than 50% in Beijing are not up to that amount. That is why the curvature did not appear to be concave as typically found with fine-mode



particles. Besides in Beijing, dust storm is very common, and it is possible that the dust events have dominated the influence of fine particles from anthropogenic sources. Throughout the considered four years, Beijing showed higher values of  $\alpha_2$  than Zinder, which can be seen from table 2. The curvature is also obvious on the curves in Figures 3a-3d. Nevertheless, in 2015, linear fit was found to be the best fit for AOD data in Zinder. This is because, the curvature in that case was found to be very small, which was considered insignificant and this necessitated the use of linear fit, instead of the polynomial fit. In this case, ~~it was concluded~~ <sup>the conclusion was</sup> that the small value of the curvature was due to bimodal aerosol size distribution, dominated by coarse mode particles [22]

Moreover, the curvature is more significant under high turbidity condition. This implies low curvature, high AOD, and high  $\alpha'$ -values. Change in curvature in spectral AOD can be due to the existence of more than one type of aerosol present in the atmosphere [22]. From Figure 3, curvature changes more rapidly in Beijing than in Zinder. This implies that in Beijing, ~~aerosol types are more than one~~ <sup>there are</sup>. This is expected in a mega-city like Beijing, with population of more than 19 million. Fine-mode aerosol particles are expected from human activities in the city, ~~coarse-mode aerosols particles are expected from dust storm~~ <sup>and</sup> which is very frequent in Beijing.

Values of  $\beta < 0.1$  signify relatively clear atmosphere, ~~whereas~~ <sup>while</sup> values of  $\beta > 0.2$  signify relatively hazy atmosphere [23]. Based on this convention, since values of  $\beta$  from Table 2 were all greater than 0.2, then ~~it was concluded~~ <sup>the conclusion was</sup> that the overall atmospheric status in both Zinder and Beijing was hazy from 2012 to 2015. From table 2, Beijing showed maximum haze status in 2012 with  $\beta$ -value 0.72 and minimum haze status in 2014 with  $\beta$ -value 0.416. On the other hands, Zinder showed maximum haze status of  $\beta$ -value 0.640 in 2012 and minimum haze status of  $\beta$ -value 0.300 in 2014.

#### 4.0 Conclusion

Based on observation and retrieval of aerosol data in two AERONET sites, in Zinder and Beijing, from 2012 to 2015, aerosol optical depth (AOD), Angstrom exponent ( $\alpha$ ), Turbidity coefficient as well as curvature of each city were analyzed and compared to ~~get~~ <sup>assess</sup> the variability and similarity of physical and optical properties of aerosol in the two cities. The results ~~found show that there is domination of coarse-mode particles in Zinder due to desert dust prevalence in all the four years of the study. The results, on the other hand, show that there is a mixture of fine-mode and coarse-mode particles in Beijing. The results also revealed that both Zinder and Beijing atmospheres were typically characterized with haze due to dust (as in the case of Zinder) and due to dust storm and excessive anthropogenic aerosol release in the atmosphere (as in the case of Beijing). In case of Zinder, the desert dust absorbs more light than it scatters, thereby causing less haze. In case of Beijing, the anthropogenic aerosols, which are dominant, scatter more light than it absorbs, thereby causing more haze in the region.~~

there are more than one aerosol types



206 5.0 References

- 207 [1] Zhou, M.G.; Liu, Y.N.; Wang, L.J.; Kuang, X.Y.; Xu, X.H.; Kan, H.D. Particulate air  
208 pollution and mortality in  
209 a cohort of chinese men. Environ. Pollut. 2014, 186, 1–6.
- 210 [2] Langrish, J.P.; Mills, N.L. Air pollution and mortality in europe. Lancet 2014, 383, 758–  
211 760.
- 212 [3] Schwartz, J.; Neas, L.M. Fine particles are more strongly associated than coarse  
213 particles with acute  
214 respiratory health effects in schoolchildren. Epidemiology 2000, 11, 6–10.
- 215 [4] Sayer, A.M.; Munchak, L.A.; Hsu, N.C.; Levy, R.C.; Bettenhausen, C.; Jeong, M.J. MODIS  
216 collection 6 aerosol products:  
217 Comparison between aqua's e-deep blue, dark target, and "merged" data sets, and usage  
218 recommendations.  
219 J. Geophys. Res. Atmos. 2014, 119, 13965–13989.
- 220 [5] Li, Z.Q.; Niu, F.; Fan, J.W.; Liu, Y.G.; Rosenfeld, D.; Ding, Y.N. Long-term impacts of  
221 aerosols on the vertical  
222 development of clouds and precipitation. Nat. Geosci. 2011, 4, 888–894.
- 223 [6] Janssen, N.A.H.; Fischer, P.; Marra, M.; Ameling, C.; Cassee, F.R. Short-term effects of  
224 PM<sub>2.5</sub>, PM<sub>10</sub> and  
225 PM<sub>2.5-10</sub> on daily mortality in the Netherlands. Sci. Total Environ. 2013, 463, 20–26.
- 226 [7] Bergen, S.; Sheppard, L.; Sampson, P.D.; Kim, S.Y.; Richards, M.; Vedal, S.; Kaufman,  
227 J.D.; Szpiro, A.A.  
228 A national prediction model for PM<sub>2.5</sub> component exposures and measurement error-  
229 corrected health effect  
230 inference. Environ. Health Perspect. 2013, 121, 1017–1025.
- 231 [8] Levy, R.C.; Mattoo, S.; Munchak, L.A.; Remer, L.A.; Sayer, A.M.; Patadia, F.; Hsu, N.C.  
232 The collection 6 MODIS  
233 aerosol products over land and ocean. Atmos. Meas. Tech. 2013, 6, 2989–3034.
- 234 [9] Remer, L.A.; Kaufman, Y.J.; Tanre, D.; Mattoo, S.; Chu, D.A.; Martins, J.V.; Li, R.R.;  
235 Ichoku, C.; Levy, R.C.;



- 236 Kleidman, R.G.; et al. TheMODIS aerosol algorithm, products, and validation. J. Atmos.  
237 Sci. 2005, 62, 947–973.
- 238 [10] Tao, M.H.; Chen, L.F.; Wang, Z.F.; Tao, J.H.; Che, H.Z.; Wang, X.H.; Wang, Y.  
239 Comparison and evaluation of  
240 the MODIS collection 6 aerosol data in China. J. Geophys. Res. Atmos. 2015, 120, 6992–  
241 7005.
- 242 [11] Dubovik, O.; Smirnov, A.; Holben, B.N.; King, M.D.; Kaufman, Y.J.; Eck, T.F.;  
243 Slutsker, I. Accuracy assessments  
244 of aerosol optical properties retrieved from aerosol robotic network (AERONET) sun and  
245 sky radiance  
246 measurements. J. Geophys. Res. Atmos. 2000, 105, 9791–9806. [CrossRef]
- 247 [12] Che, H.; Shi, G.; Uchiyama, A.; Yamazaki, A.; Chen, H.; Goloub, P.; Zhang, X.  
248 Intercomparison between  
249 aerosol optical properties by a prede skyradiometer and cimel sunphotometer over  
250 Beijing, China.  
251 Atmos. Chem. Phys. 2008, 8, 3199–3214.
- 252 [13] Eck, T.F.; Holben, B.N.; Dubovik, O.; Smirnov, A.; Goloub, P.; Chen, H.B.; Chatenet,  
253 B.; Gomes, L.; Zhang, X.Y.;  
254 Tsay, S.C.; et al. Columnar aerosol optical properties at aeronet sites in central Eastern  
255 Asia and aerosol  
256 transport to the tropical Mid-Pacific. J. Geophys. Res. Atmos. 2005, 110.
- 257 [14] Schuster, G.L.; Vaughan, M.; MacDonnell, D.; Su, W.; Winker, D.; Dubovik, O.;  
258 Lapyonok, T.; Trepte, C.  
259 Comparison of calipso aerosol optical depth retrievals to aeronet measurements, and a  
260 climatology for the  
261 lidar ratio of dust. Atmos. Chem. Phys. 2012, 12, 7431–7452.
- 262 [15] Garcia, O.E.; Diaz, J.P.; Exposito, F.J.; Diaz, A.M.; Dubovik, O.; Derimian, Y.;  
263 Dubuisson, P.; Roger, J.C.  
264 Shortwave radiative forcing and efficiency of key aerosol types using aeronet data.  
265 Atmos. Chem. Phys. 2012, ~~Add test of reference here~~  
266 [12] 5129–5145.



- 267 [16] Lee, J.; Kim, J.; Yang, P.; Hsu, N.C. Improvement of aerosol optical depth retrieval  
268 from MODIS spectral  
269 reflectance over the global ocean using new aerosol models archived from aeronet  
270 inversion data and tri-axial  
271 ellipsoidal dust database. *Atmos. Chem. Phys.* 2012, 12, 7087–7102.
- 272 [17] Mi, W.; Li, Z.; Xia, X.; Holben, B.; Levy, R.; Zhao, F.; Chen, H.; Cribb, M. Evaluation of  
273 the moderate resolution  
274 imaging spectroradiometer aerosol products at two aerosol robotic network stations in  
275 China. *J. Geophys.*  
276 *Res. Atmos.* 2007, 112.
- 277 [18] Zhang, A.; Qi, Q.; Jiang, L.; Zhou, F.; Wang, J. Population exposure to PM<sub>2.5</sub> in the  
278 urban area of Beijing.  
279 *PLoS ONE* 2013, 8, e63486. SONE T
- 280 [19] Xie, Y.; Li, Z.; Li, D.; Xu, H.; Li, K. Aerosol optical and microphysical properties of  
281 four typical sites of sonet  
282 in China based on remote sensing measurements. *Remote Sens.* 2015, 7, 9928–9953.
- 283 [20] Dubovik, O.; Holben, B.; Eck, T.F.; Smirnov, A.; Kaufman, Y.J.; King, M.D.; Tanre, D.;  
284 Slutsker, I. Variability of  
285 absorption and optical properties of key aerosol types observed in worldwide locations.  
286 *J. Atmos. Sci.* 2002,  
287 59, 590–608.
- 288 [21] Wei Chen, Hongzhao Tang, Haimeng Zhao 3 and Lei Yan, Analysis of Aerosol  
289 Properties in Beijing Based on  
290 Ground-Based Sun Photometer and Air Quality  
291 Monitoring Obs *Remote Sens.* 2016, 8, 110; doi:10.3390/rs8020110, observations from  
292 2005 to 2014.
- 293 [22] D. G. Kaskaoutis and H. D. Kambezidis, Investigation into the wavelength  
294 dependence of the aerosol optical depth  
295 in the Athens area, *Q. J. R. Meteorol. Soc.* (2006), 132, pp. 2217–2234
- 296 [23] D.O. Akpootu and M. Momoh, The Ångström Exponent and Turbidity of Soot  
297 Component

298 in the Radiative Forcing of Urban Aerosols, Nigerian Journal of Basic and Applied  
299 Science (March, 2013), 21(1): 70-78